



Alternatively spliced down syndrome cell adhesion molecule (Dscam) controls innate immunity in crab

Received for publication, July 17, 2019, and in revised form, September 12, 2019. Published, Papers in Press, September 19, 2019, DOI 10.1074/jbc.RA119.010247

Dan Li^{#1}, Zhicheng Wan^{#1}, Xuejie Li⁵, Ming Duan[¶], Lei Yang[‡], Zechao Ruan[‡], Qun Wang^{#2}, and Weiwei Li^{#3}

From the [‡]State Key Laboratory of Estuarine and Coastal Research, Laboratory of Invertebrate Immunological Defense and Reproductive Biology, School of Life Sciences, East China Normal University, Shanghai 200241, the ⁵College of Fisheries and Life Science, Dalian Ocean University, Dalian 116023, and the [¶]State Key Laboratory of Freshwater Ecology and Biotechnology, Institute of Hydrobiology, Chinese Academy of Sciences, Wuhan 430072, China

Edited by Luke O'Neill

Alternatively-spliced hypervariable immunoglobulin domain-encoding molecules, called Down syndrome cell adhesion molecule (Dscam), have been widely detected as components of the arthropod immune system. Although its ability to specifically bind pathogens and enable phagocytosis of bacteria has been elucidated, the signal transduction mechanisms or effectors that activate post-Dscam-binding pathogens remain poorly characterized. Here, we reveal the alternative splicing exons of Dscam's cytoplasmic tail and its isoforms in the hemocytes of crab (*Eriocheir sinensis*), showing that the expression of Dscam was acutely induced after an immune challenge, which suggested its functioning for innate immunity. Significantly decreased expression levels of antimicrobial molecular peptides (AMPs) were detected in Dscam-silenced crab hemocytes *in vitro*, which coincided with their vulnerability to infection by *Staphylococcus aureus* and higher bacterial concentrations occurring in Dscam-silenced crabs *in vivo*. Further experimental investigation demonstrated that Dscam-regulated AMP expression via the Src homology (SH)3-binding domain in the first constant exon translated protein of the cytoplasmic tail bound with the SH3 domain of the Dock, an SH3/SH2 adaptor protein required for axon guidance. Dock promoted extracellular signal-regulated kinase (ERK) phosphorylation via indirect binding and then regulated dorsal phosphorylation and translocation from the cytoplasm to the nucleus, subsequently promoting AMP expression for the effective removal of bacteria. To the best of our knowledge, this comprehensive study is the first to highlight the critical role of the alternatively-spliced Dscam cytoplasmic tail in antimicrobial control activity. It also suggests possible crosstalk occurring between Dscam and other pattern recognition receptors.

The Down syndrome cell adhesion molecule (Dscam)⁴ belongs to novel members of the immunoglobulin superfamily due to shared structural features with Igs (1, 2). Dscam functions in the differentiation of the nervous system (1) and in the recognition and binding activity of the innate immune reaction in animals (2). Throughout the metazoa, Dscam's domain composition and physical arrangement has remained identical, namely 9(Ig)-4(fibronectin, FN)-1(Ig)-2(FN) (3). The most striking characteristic of Dscam is its alternative splicing ability, which can potentially generate 38,016 different isoforms through mutually exclusive splicing of four cassette exon clusters in *Drosophila melanogaster* (1, 4). Furthermore, additional sources of diversity were also identified in the cytoplasmic tail (3, 5, 6), which may generate even more Dscam isoforms. Alternative splicing is an ancient and widespread mechanism used by eukaryotic organisms to enhance protein diversity and regulate gene expression (7). For example, up to 95% of the primary transcripts in humans are thought to undergo alternative splicing (8), which may contribute to subsequent functional differentiation among cells.

The extensive somatic diversification of their immune receptors is a hallmark of higher vertebrates (9, 10). Nevertheless, recent studies have demonstrated the critical role of Dscam alternatively-spliced isoforms in providing immune protection for insects (4). *In vivo* silencing of Dscam reduced phagocytic ability and led to a proliferation of opportunistic bacteria, even in the hemolymph of unchallenged mosquitoes, which together suggested Dscam's key involvement in anti-bacterial immunity. Interestingly, after mosquito Sau5B cells were infected with bacteria, pathogen-induced Dscam showed a high-binding affinity against the originally induced bacteria, whereas specific Ig2 variant-Dscam isoform-silenced mosquitoes became more susceptible to infection when challenged with the same bacteria (4). Collectively, the body of research to date suggests a potentially critical role played by Dscam in constituting specific anti-bacterial immune responses. Furthermore, *in vivo* overexpression of parasite-specific Dscam isoforms was able to augment the mosquitoes' resistance to particular parasites, while *in vivo*

This work was supported by National Natural Science Foundation of China Grants 31602189 (to W. L.) and 31672639 (to Q. W.) and National Key R&D Program of China Grants 2018YFD0901701 and 2018YFD0900605. The authors declare that they have no conflicts of interest with the contents of this article.

This article contains Figs. S1–S5 and Table S1.

¹ Both authors contributed equally to this work.

² To whom correspondence may be addressed. E-mail: qwang@bio.ecnu.edu.cn.

³ To whom correspondence may be addressed. E-mail: wqli@bio.ecnu.edu.cn.

⁴ The abbreviations used are: Dscam, Down syndrome cell adhesion molecule; AMP, antimicrobial molecular peptide; AMP, antimicrobial peptide; SH, Src homology; FN, fibronectin; ERK, extracellular signal-regulated kinase; DAPI, 4',6-diamidino-2-phenylindole dihydrochloride; qRT, quantitative RT; JNK, c-Jun N-terminal kinase; co-IP, co-immunoprecipitation; ITIM, immunoreceptor tyrosine-based inhibitory motif.

silencing of a *Plasmodium*-specific isoform rendered the mosquitoes more susceptible to the parasite; those findings indicated specific Dscam isoforms may also contribute to immunity against parasites as well (4, 11). Taken together, the evidence clearly supports the view that Dscam alternatively-spliced isoforms could specifically bind to different pathogens, leading to subsequent well-known immune reactions such as phagocytosis (2).

Yet, compared with the alternatively spliced Ig domains in Dscam, little is known about how its cytoplasmic tail may contribute to immune protection. Undoubtedly, far fewer alternatively spliced isoforms are derived in the cytoplasmic tail than Ig domains due to the generally limited exons in this region; but the combination of alternatively-spliced exons in Dscam cytoplasmic tails may provide an efficient mechanism by which different signal transduction pathways and functions are triggered following pathogen-specific binding events in immune responses.

In this respect, to date the best-studied and understood Dscam function is phagocytosis regulation in cellular immunity, now widely confirmed in different arthropods by multiple research groups (2, 4, 12). In contrast, whether Dscam can trigger an immune signaling pathway that contributes to humoral immunity, such as that achieved by antimicrobial peptides (AMPs) via the alternatively-spliced cytoplasmic tail, is a far from resolved issue. In this study, we show the genomic structure of Dscam's cytoplasmic tail in crab, test the immune protection role of Dscam in a bacterial challenge, identify the AMPs whose expression regulates Dscam both *in vivo* and *in vitro*, and uncover a novel antimicrobial-signaling pathway activated by the cytoplasmic tail of Dscam. As far as we know, this is the first reported evidence of a Dscam-triggered immune signaling pathway in nature.

Results

Gene structure and expression pattern of Dscam

The transmembrane region and cytoplasmic tail were both unique in the membrane-bound Dscam compared with soluble Dscam (2). Previous studies focused on alternative splicing exons in the Ig domain that are shared by membrane-bound and soluble Dscam (2, 4, 13, 14); however, information about the alternatively-spliced cytoplasmic tail still remains limited. To resolve this outstanding issue, the gene structure of Dscam was determined through whole-genome sequencing of *Eriocheir sinensis*,⁵ followed by the exons' predicting and cloning of many cDNAs. Results revealed nine exons in the cytoplasmic tail of Dscam, named exons 32–40 (Fig. S1), followed by the 31 exons in the outer membrane region. This cytoplasmic tail can generate four isoforms (Fig. S2), including exons 32–40, 35^{-/-}–36^{-/-}, 33^{-/-}, and 33^{-/-}–35^{-/-}–36^{-/-} by the alternatively spliced exons 33 and 35/36, while the signature domain of the SH3- and SH2-binding domains were located in the constant exons 32 and 37. The signature motif of endocytosis, polyproline, and ITIM-like were located in alternatively spliced exon 33, constant exon 38, and constant exon 40, respectively (Fig. 1A). The

phylogenetic analysis demonstrated that the Dscam of crustaceans had diverged from that of insects, albeit the relationship of the two *Daphnia* species' Dscam was ambiguous. Moreover, the *EsDscam* clustered with another mud crab, *Scylla paramamosain*, which formed a sister group with other crustaceans (Fig. 1B).

To investigate the expression profiles of Dscam isoforms, primers were designed across constant exon 37 and exon 38 as it is shared between all membrane-bound Dscam (Fig. 1C). The LPS (Fig. 1D) and *Staphylococcus aureus* (Fig. 1, E and F) challenge induced high expression levels of Dscam, both *in vitro* and *in vivo*, and its expression peaked at 24 h post-*S. aureus* infection *in vitro* (Fig. 1E) and 12 h post-*S. aureus* stimulation *in vivo* (Fig. 1F). 24 h since the primary cultured hemocytes of *E. sinensis* was *S. aureus*-stimulated, the expressions of 10 AMPs (ALF1, ALF2, ALF4, LYZ1, LYZ2, LYZ3, LYZ4, Crus1, Crus3, and DWD) were also significantly induced (Fig. 1G). This result pointed to a possible linkage between Dscam and the expression of AMPs.

Dscam control of antimicrobial activity in crab

To test the possibility of Dscam regulated AMPs expression, dsRNA that targeted constant exon 32 was transfected into primary-cultured *E. sinensis* hemocytes to suppress the expression of membrane-bound Dscam isoforms (Fig. 2A). The expression of Dscam was significantly inhibited by this dsRNA transfection (Fig. 2B), followed by significantly reduced AMPs' expression (namely ALF1, ALF2, ALF4, LYZ1, LYZ3, LYZ4, Crus1, and DWD) upon *S. aureus* stimulation (Fig. 2C).

To elucidate the role of Dscam *in vivo*, crabs were injected with dsGFP or dsDscam for 12 h and then received an *S. aureus* infection and were injected with dsRNA again at day 2 to extend the effect of RNAi. Crab survival was monitored from days 1 to 4, and bacterial CFU were analyzed at day 3 (Fig. 2D). Dscam mRNA and protein expression were significantly knocked down by the dsRNA injection for at least 3 days (Fig. 2E), accompanied by significantly reduced survival (Fig. 2F), as well as significantly increased bacterial concentration in the hemolymph compared with the dsGFP-treated group of crabs (Fig. 2G). Together, this suggested Dscam might control antimicrobial activity of crab via regulation of AMPs.

Dscam regulated the signaling pathway that led to expression of AMPs

The crucial role of the Toll pathway in regulating AMPs' expression following Gram-positive bacterial infection of invertebrate species has been widely confirmed (15). Hence, we speculated Dscam likewise regulated AMPs' expression in crab; a hypothesis tested here by knocking it down *in vitro*. Not only was dorsal phosphorylation obviously reduced when compared with the siGFP-treated group (Fig. 3A and Fig. S5A), the dorsal translocation from cytoplasm to nucleus was also suppressed in the Dscam-silenced hemocytes (Fig. 3B), which is consistent with Dscam regulating the Toll pathway. ERK reportedly promotes dorsal translocation (16), so we also considered whether Dscam could regulate the MAPK/ERK pathway. To test this, the phosphorylation and total protein levels of ERK and JNK were determined, which demonstrated a clearly inhibited ERK

⁵ D. Li, X. Li, Q. Wang, and W. Li, unpublished observations.

Dscam controls innate immunity in crab

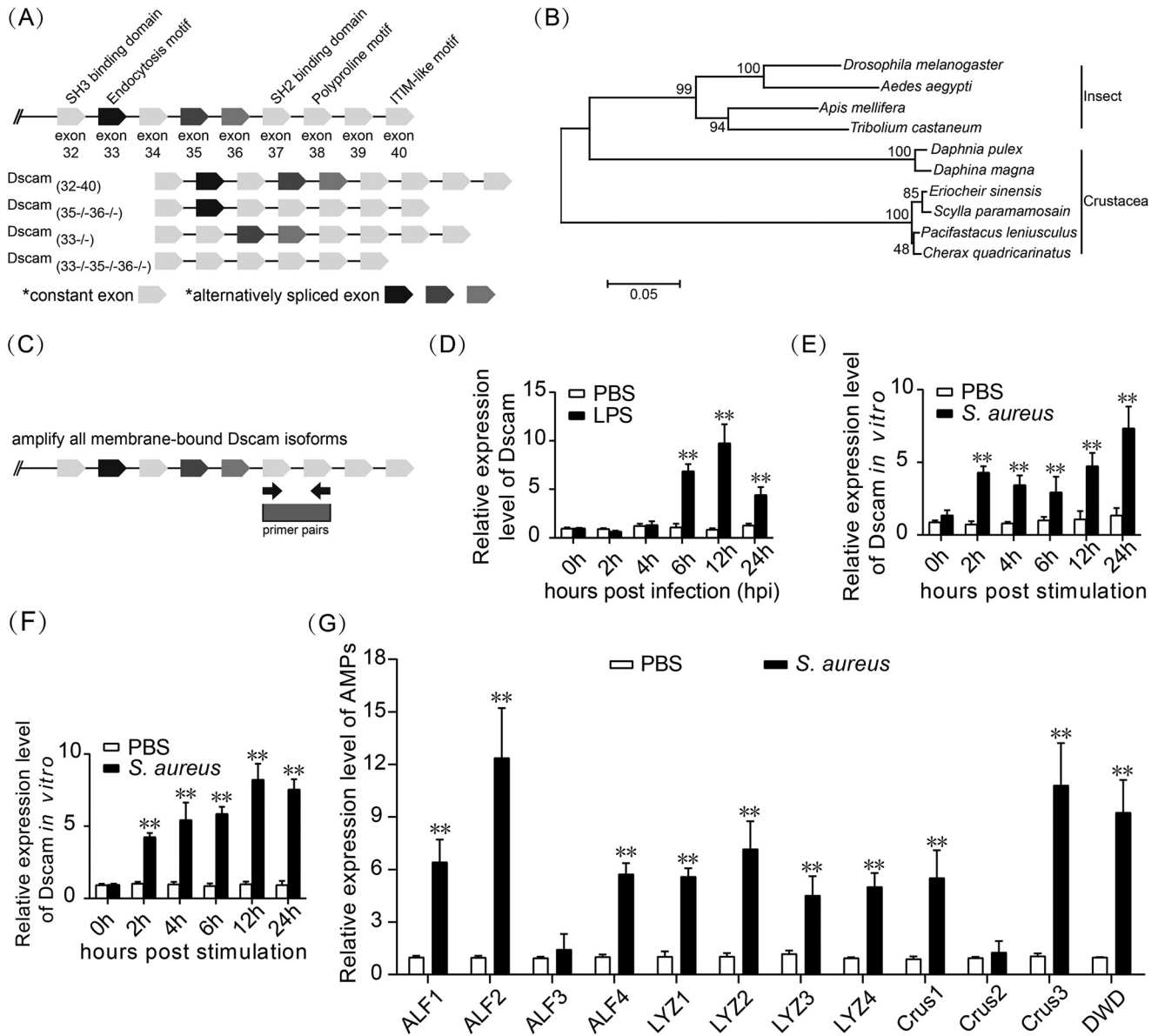


Figure 1. Expression of Dscam and antimicrobial peptides when challenged with *S. aureus*. A, schematic illustration of Dscam's cytoplasmic tail genomic DNA structure in *E. sinensis* crab. The transmembrane region, exons, intron, SH3-binding domain, endocytosis motif, SH2-binding domain, and ITIM/ITAM (immunoreceptor tyrosine-based activation motif) motifs are illustrated. The respective structure of four different Dscam tail isoforms is displayed below, wherein the sites for constant and alternatively spliced exons are color-coded. B, phylogenetic analysis based on multiple alignments of *EsDscam* and other membrane-bound Dscam proteins according to a neighbor-joining phylogenetic tree ($n = 1000$ bootstrap replications), with numerical robustness given at the branch nodes. C, pair of primers amplified the Dscam cytoplasmic tail constant exon 32, designed to detect the expression of all membrane-bound Dscam isoforms. D–F, expression of Dscam in crab hemocyte was assessed by qRT-PCR on a time-course post-challenge (with LPS and *S. aureus*), both *in vitro* and *in vivo*. Bars are the mean \pm S.D. from three replicate samples, with at least five crabs per sample. G, expression profiles of antimicrobial peptides' mRNA in crab hemocyte following the *S. aureus* challenge. Bars are the mean \pm S.D. from three replicate samples, with at least five crabs per sample. **, $p < 0.01$ (Student's *t* test).

phosphorylation rate, as well as a total ERK protein level in Dscam-silenced hemocytes at both the 30- and 60-min post-*S. aureus* stimulation (Fig. 3C and Fig. S5B) that was supported by the suppressed p-ERK fluorescent signal in Dscam-silenced hemocytes (Fig. 3D). Unfortunately, antibody-binding sites of the commercial p-38 antibody shared low similarities with p-38 in crab, and the specific *E. sinensis* p-38 antibody could not be synthesized, hence their omission in this study.

ERK regulates expression of AMPs via the Toll pathway

To test whether ERK could regulate AMPs expression, ERK was knocked down in crab hemocytes (Fig. 4A). Doing

so significantly decreased the expression of AMPs (ALF1, ALF2, ALF4, LYZ1, LYZ3, LYZ4, Crus1, and DWD) detected before as regulated by Dscam upon *S. aureus* stimulation, when compared with the siGFP-treated group (Fig. 4B). We further speculated that ERK may regulate AMPs' expression via dorsal. To test this hypothesis, ERK phosphorylation was inhibited by the MEK1/2 inhibitor PD98059, and the 10 μ M concentration clearly affected ERK phosphorylation inhibition (Fig. 4C and Fig. S5C); moreover, this concentration also produced a conspicuous effect after the *S. aureus* stimulation (Fig. 4D and Fig. S5D). By using the ERK phosphorylation inhibition system, reduced dorsal phosphorylation was

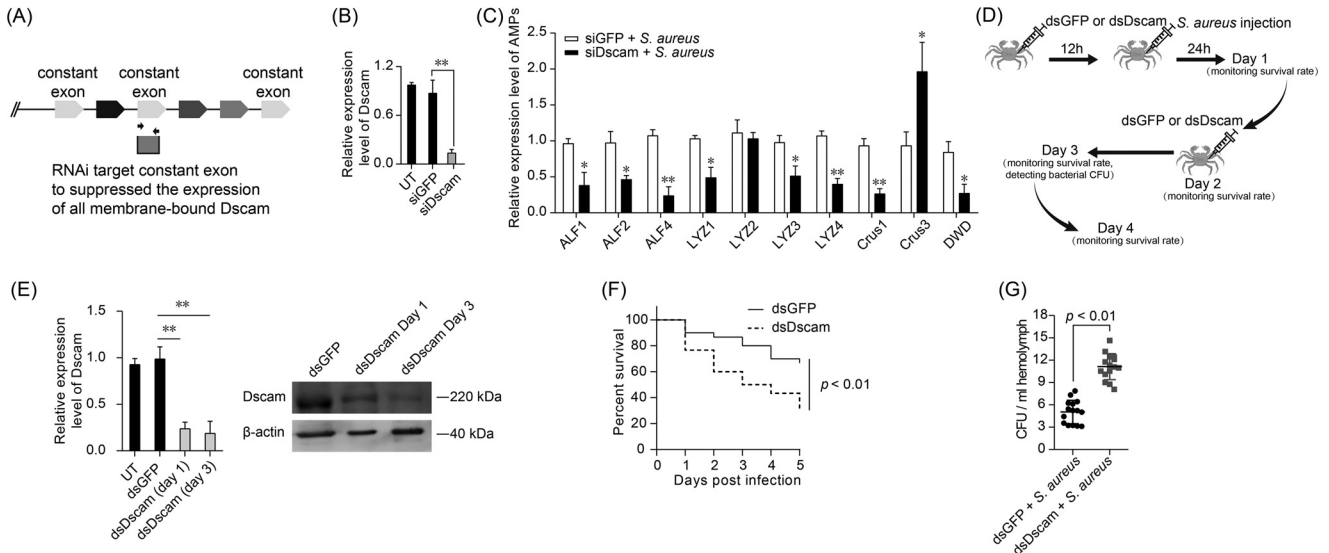


Figure 2. Protecting crab hosts from *S. aureus* infection by Dscam. *A*, Dscam siRNA (*siDscam*) primers targeting the cytoplasmic tail constant exon 34 designed to knock down membrane-bound Dscam isoforms. *B*, effects of RNAi on Dscam expression in crab hemocyte, determined 24 h post-transfection with *siDscam* by qRT-PCR. *Bars* are the mean \pm S.D. from three replicate samples, with at least three crabs per sample. *C*, knockdown of Dscam reduced expression of multiple AMPs in the hemocyte upon *S. aureus* challenge. *Bars* are the mean \pm S.D. from three replicate samples, with at least five crabs per sample. *D*, timeline overview of host protection from *S. aureus* infection by RNAi Dscam in crab. *E*, RNAi efficacy of Dscam in juvenile crabs injected with 1 μ g/g dsRNA, with Dscam expression analyzed from at days 1 and 3 post-injection by qRT-PCR and Western blotting. *Bars* are the mean \pm S.D. from three replicate samples, with at least five crabs per sample. The Western blotting data shown are from three independent repeats. *F*, knockdown of Dscam led to the death of crabs injected with 15 μ g of dsDscam each; their survival was recorded for 4 days from three replicate samples with at least 10 crabs per sample. *G*, RNAi of Dscam increased *S. aureus* proliferation crabs treated as described above; the hemolymph was drawn out at day 3 post-*S. aureus* infection and plated onto agar plates, and bacterial counts were determined. Where applicable, dsGFP = control. **, $p < 0.01$; *, $p < 0.05$ (Student's *t* test).

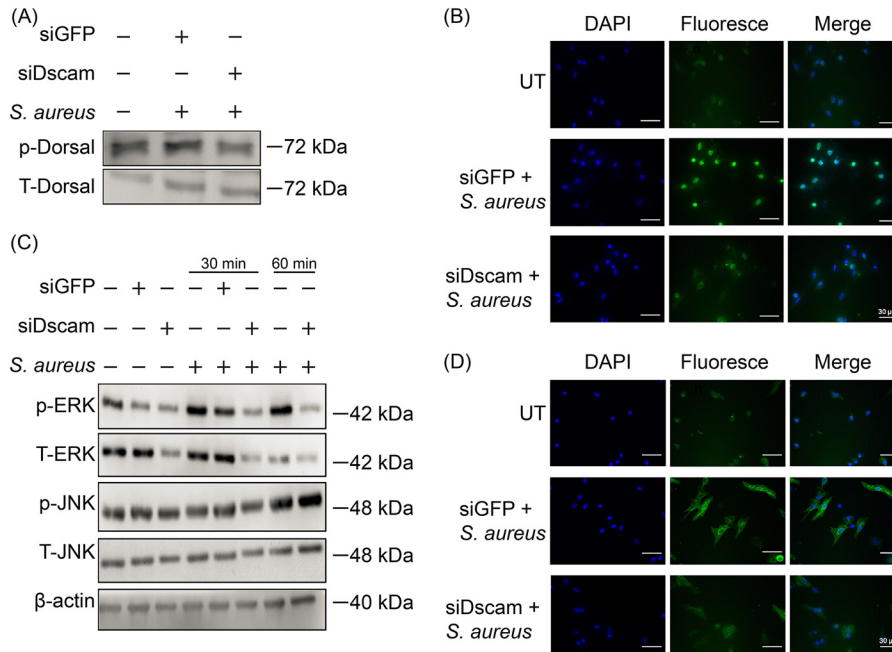


Figure 3. Dscam regulates the Toll-signaling pathway and phosphorylation of ERK in crab hemocyte. *A*, knockdown of Dscam suppressed phosphorylated dorsal upon *S. aureus* challenge in a Western blotting. *B*, Dscam RNAi suppressed translocation of phosphorylated dorsal after *S. aureus* stimulation in crab hemocyte, as detected by immunocytochemical staining. The green fluorescence signal indicated the distribution of phosphorylated dorsal, whereas blue indicated hemocytes' nucleus stained with DAPI. *C*, knockdown of Dscam reduced both total ERK and phosphorylated ERK expression in crab hemocytes after 30 or 60 min of *S. aureus* stimulation, but not JNK, in the Western blotting. *D*, Dscam RNAi reduced phosphorylated ERK in both the cytoplasm and nucleus following *S. aureus* stimulation, as detected by immunocytochemical staining. The green fluorescence signal indicated the distribution of phosphorylated ERK, whereas blue indicated the nuclei of hemocytes stained with DAPI. All data shown are from three independent experimental repeats. Where applicable, siGFP or siGFP plus stimulation served as the control.

found compared with the inhibitor-treated group (Fig. 4E and Fig. S5E). To verify this result in mRNA levels, ERK was knocked down in hemocytes followed by *S. aureus* stim-

ulation, and reduced dorsal phosphorylation was confirmed compared with the siGFP-treated group (Fig. 4F and Fig. S5F).

Dscam controls innate immunity in crab

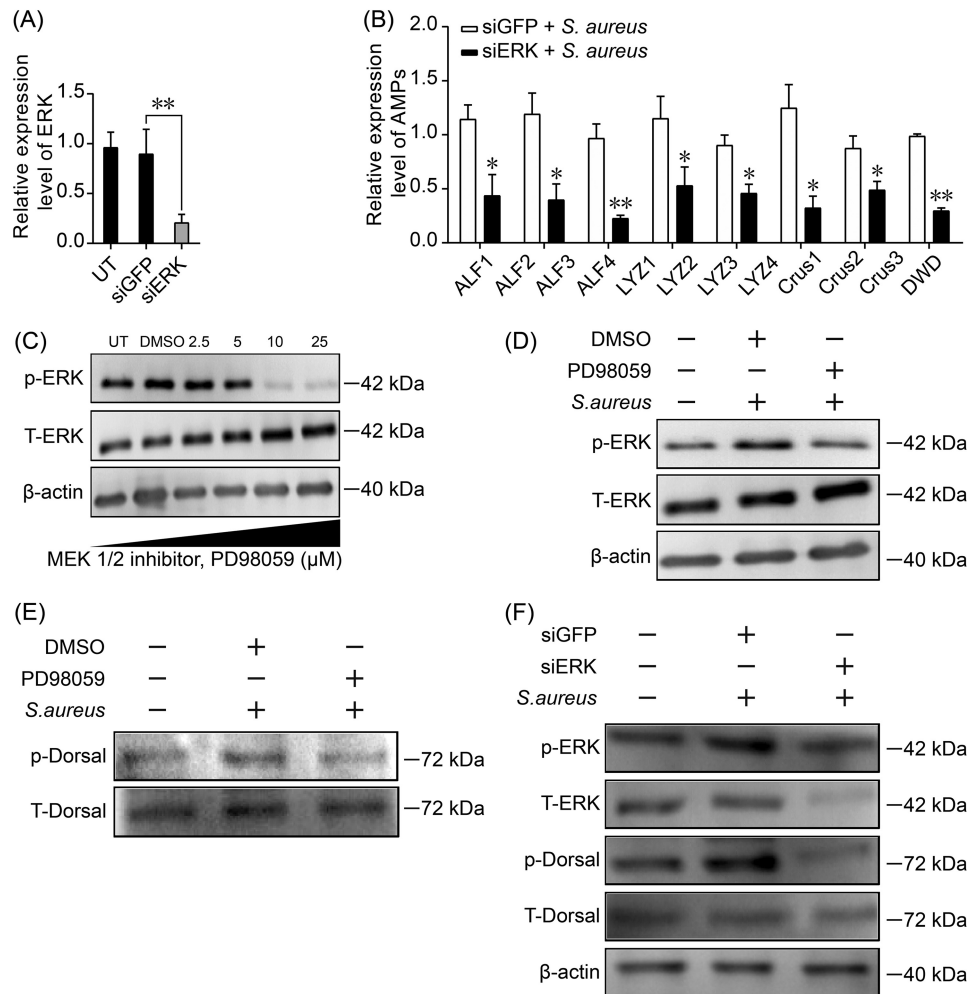


Figure 4. ERK affects Toll signaling in crab hemocytes. *A*, effects of ERK RNAi in crab hemocytes. The expression of ERK in hemocytes was determined at 24 h after their transfection with siERK, by qRT-PCR (dsGFP was used as control). *B*, qRT-PCR was used to determine the expression of AMPs in the Dscam-silenced hemocytes after *S. aureus* stimulation. The data shown are from three independent experimental repeats, with the mean \pm S.D. given in the panels. *C*, Western blotting detected the reduced phosphorylation of ERK after injection of PD98059 at a dose course (2.5, 5, 10, and 25 μ M) at 1 h. *D*, Western blotting detected the reduced phosphorylation of ERK after injection of PD98059 for 30 min and stimulation with *S. aureus* for another 30 min. *E*, Western blotting detected the reduced phosphorylation of dorsal after injection of PD98059 and stimulated with *S. aureus*. *F*, knockdown of ERK reduced expression of both ERK and dorsal phosphorylation after *S. aureus* stimulation, according to the Western blotting. The Western blotting data shown are from three independent repeats. Where shown, *, $p < 0.05$; **, $p < 0.01$ (Student's *t* test).

Dock regulates antimicrobial activities

That Dock protein binds with Dscam in neuron cells is known (1), so we investigated the effect of Dock in Dscam-regulated ERK phosphorylation because the immune functions of Dock have not been reported. To test whether Dock regulated innate immunity in crab, the cDNA full-length of the *Dock* gene in *E. sinensis* was cloned (Fig. S3), and its bioinformatics analysis suggested three SH3 domains and one SH2 domain in the Dock protein, with the Dock protein highly similar within the arthropod species (Fig. 5A and Fig. S4). The expression level of *Dock* was significantly induced post-*S. aureus* stimulation in hemocytes, especially at 12 h (Fig. 5B), which indicated its immune functioning in crab. Next, siRNA was transfected into hemocytes for the RNAi *Dock* expression (Fig. 5C). Compared with the siGFP-treated group, this resulted in a clearly decreased ERK phosphorylation signal in hemocytes (Fig. 5D), a suppressed dorsal translocation from cytoplasm to nucleus (Fig. 5E), and significantly reduced AMPs' expression levels regulated by Dscam in *Dock*-silenced hemocytes upon *S. aureus*

stimulation (Fig. 5F). Collectively, these results suggested Dock could regulate AMPs expression via ERK/dorsal signaling in the crab.

Dscam binding with Dock

The SH3-binding domain in Dscam may act as a potential target for the SH3 domain in Dock to affiliate with it (1). To elucidate how binding might occur between Dscam and Dock, the full-length of Dock and four truncated Dscam cytoplasmic tail cDNA plasmids (consisting of all constant exons for 891 bp, exon 33–36/38–40 for 807 bp, exon 34/37–40 for 720 bp, and full-length for 1182 bp) were constructed and transfected into HEK293T cells (Fig. 6A). The co-IP results demonstrated that each plasmid was well-expressed in these cells; the full-length Dscam cytoplasmic tail (FLAG-1182) could strongly bind with the Dock protein; all constant exons containing the isoform (FLAG-891) had a strong binding activity with the Dock protein; isoform without a constant exon 32 and exon 37 (FLAG-807) was unable to bind with the Dock protein; isoform con-

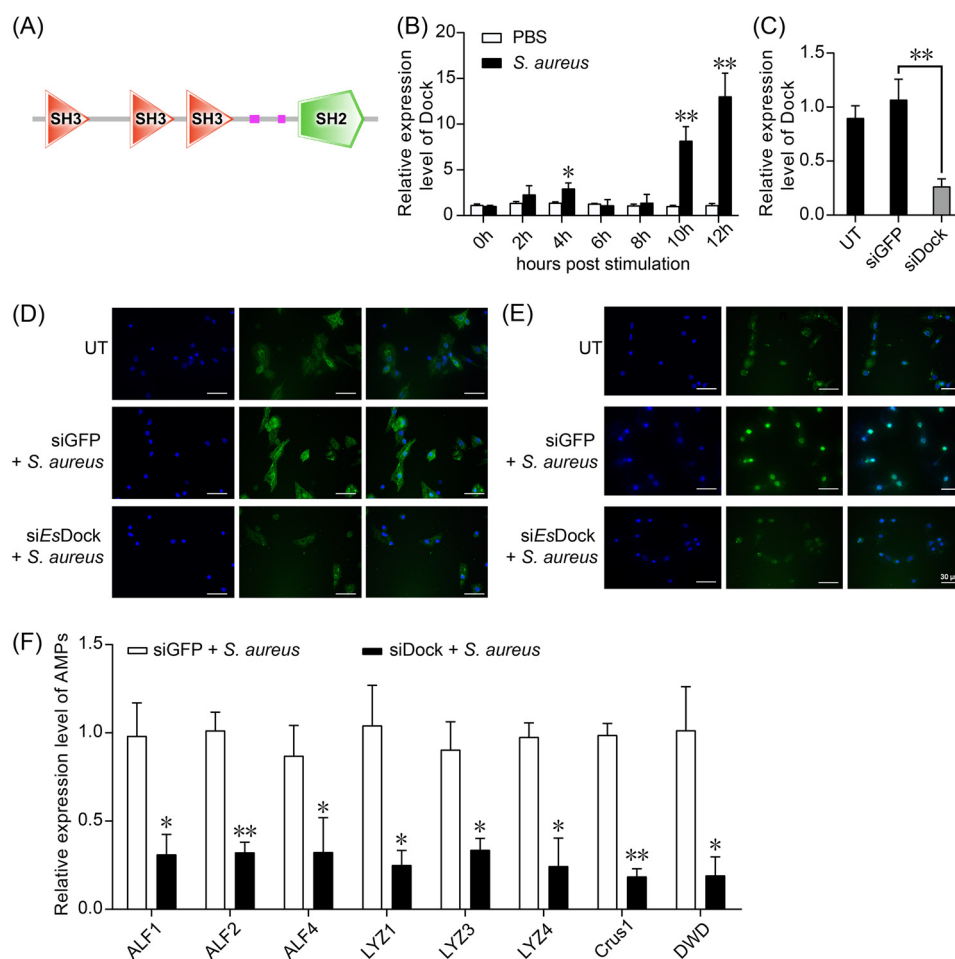


Figure 5. Role of Dock in antibacterial immune reactions. *A*, domain architectures of the Dock protein in crab (upper), illustrating its three SH3-binding domains, and one SH2-binding domain. *B*, expression of Dock detected in the crab hemocytes stimulated with *S. aureus* over the time course. *C*, effects of Dock RNAi in crab hemocytes, in which the expression of Dock was determined 24 h after their transfection with siDock, by qRT-PCR (siGFP = control). *D*, Dock RNAi suppressed ERK phosphorylation in *S. aureus*-stimulated hemocytes, as detected by immunocytochemical staining. *E*, Dock RNAi suppressed translocation of dorsal in *S. aureus*-stimulated hemocytes, as detected by immunocytochemical staining. *F*, qRT-PCR was used to detect the expression of AMPs in the Dock-silenced hemocytes after *S. aureus* stimulation. *D* and *E*, green fluorescence signal indicates the distribution of phosphorylated ERK and dorsal, respectively, whereas blue indicates the nuclei of hemocytes stained with DAPI (siGFP with *S. aureus* stimulation = control). Bars are the mean \pm S.D. from three independent experimental repeats. Where shown, *, $p < 0.05$; **, $p < 0.01$ (Student's *t* test).

taining all constant exons without exon 32 (FLAG-720) had weak binding activity with the Dock protein. Together, this showed the SH3-binding domain in the constant exon-translated protein of Dscam cytoplasmic tail can bind to the SH3 domain of Dock.

Dock regulates ERK phosphorylation via indirect binding

We then wondered whether Dock could regulate the phosphorylation of ERK, as this would enable it to later participate in the process of Dscam-regulated antimicrobial activities. To test this, Dock was knocked down in hemocytes, for which the Western blotting results showed an obviously reduced ERK phosphorylation at both 30 and 60 min post-*S. aureus* stimulation (Fig. 6C and Fig. S5G). Moreover, both Dock and ERK plasmids were transfected into S2 cells for overexpression, which resulted in a greater ERK phosphorylation rate in Dock-overexpressed cells (Fig. 6D and Fig. S5H). In sum, these results demonstrated Dock regulated ERK phosphorylation. To explore whether Dock did so via direct binding, the plasmids of these two genes were transfected into HEK293T cells, but the

co-IP results revealed no evidence for direct binding (Fig. 6E). Moreover, this result was confirmed by co-immunoprecipitation assay by using a specific antibody against *Es*ERK and *Es*Dock in *E. sinensis* hemocytes (Fig. 6F).

Discussion

The Dscam gene is an extraordinary example of biomolecular diversity; by combining alternatively spliced exons, thousands of isoforms can be produced from this single gene (1, 17, 18). Such diversity has so far only been found in insects and crustaceans (19), and its essential involvement in neural networks' wiring is now well-characterized for *D. melanogaster* (20). Pioneering studies of multiple arthropod species provide convincing evidence that Ig domains in the outer membrane region of Dscam specifically bind to pathogens, subsequently activating phagocytosis in hemocytes (2, 4). These exciting findings showed that via processes of somatic diversification, arthropod species harbor an unexpectedly great potential diversity of immune molecules. Here, we hypothesized Dscam

Dscam controls innate immunity in crab

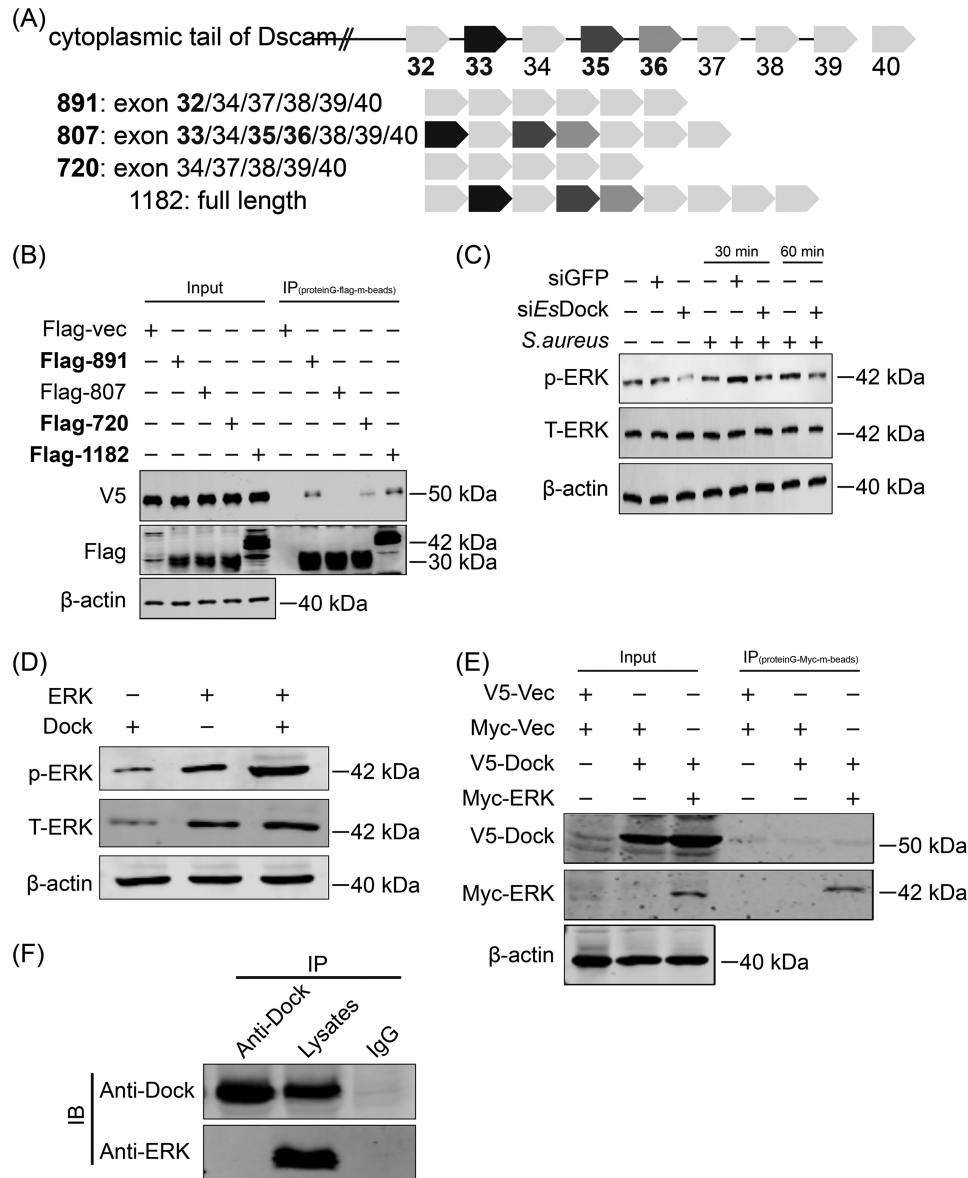


Figure 6. Dock affinity with Dscam and regulation of ERK phosphorylation via indirect binding. *A*, illustration of the truncated membrane of the Dscam cytoplasmic tail protein. *B*, co-immunoprecipitation (IP) assay showed the interaction between differently-truncated Dscam cytoplasmic tail proteins and Dock in HEK293T cells. Anti-V5 and anti-FLAG antibodies were used to detect Dock and truncated Dscam isoforms in co-infected HEK293T cells, respectively. The anti-V5 and anti-FLAG antibodies were incubated with the cell lysates and then isolated using Protein G-FLAG-m-beads. *C*, Western blotting detected the reduced phosphorylation of ERK in Dock-silenced crab hemocytes stimulated by *S. aureus* at 30 and 60 min, respectively (siGFP = control). *D*, ERK phosphorylation increased in cultured S2 cells overexpressing both Dock and ERK proteins. *E* and *F*, co-immunoprecipitation (IP) assay did not show any interaction between Dock and ERK protein both in the HEK293T cells (*E*) and crab hemocytes (*F*). *B* and *E*, anti-V5 and anti-Myc antibodies were used to detect Dock and ERK in co-infected HEK293T cells, respectively. The anti-V5 and anti-FLAG antibodies were incubated with the cell lysates and then isolated using Protein G-FLAG-m-beads. The data shown are from three independent experimental repeats.

could provide the mechanistic underpinnings of such specific immune responses.

As a pathogen recognition receptor, the cytoplasmic tail of membrane-bound Dscam provides the structural basis for signaling transduction upon receiving dangerous signals by Ig domains situated in the outer membrane region. Surprisingly, however, this process has not been investigated in previous studies. Dscam isoforms with different cytoplasmic tails were identified in some species, such as *D. melanogaster* (5), *Daphnia magna* (3), and *Penaeus monodon* (6), with varied patterns of alternative splicing. For example, the four cytoplasmic tail variants found in *D. magna* arise from the inclusion or exclu-

sion of exons 27 and 30, and the latter's absence would shift the downstream reading frame (3). Similarly, four cytoplasmic tail variants were also found in *D. melanogaster* due to the presence or absence of exons 19 and 23, with the downstream reading frame shifted if exon 23 was excluded from mature mRNA (5). By contrast, in crab Dscam, there are two individually spliced exon regions leading to four cytoplasmic tail isoforms, no matter which exon is excluded, so the downstream reading frame remains unchanged. Similarly, the combination of six diverse elements (putative exons) led to different cytoplasmic tail isoforms in *P. monodon*, whose downstream reading frame is unaffected by a sequence deletion (6). The diverse functional

motifs in such exons might be associated with different signal transduction pathways, perhaps corresponding to the neuron development and immune response functions of Dscam. In a study of *Drosophila* neuronal morphogenesis, when compared with the full-length endodomain, those isoforms without exons 19 and 23 played a more important role in post-embryonic stages (5). For immune reactions, however, the functions of spliced exons and endodomains in the cytoplasmic tail of *EsDscam* and even among well-studied arthropods are unknown.

Dock is an adaptor protein containing three SH3 domains and a single SH2 domain, and it is closely related to mammalian Nck (21, 22). Dock mutants often show defects in axon guidance in the adult fly's visual system and its embryonic nervous system (1). In previous studies of *D. melanogaster*, Dscam was isolated by virtue of its affinity to Dock, in that Dscam can directly and strongly bind to its SH3 domain but only early to its SH2 domain (1). Genetic studies have revealed that Dscam, Dock, as well as Pak, a serine/threonine kinase, may act together to direct path-finding of Bolwig's nerve, which contains a subclass of sensory axons, to an intermediate target in the embryo (1). Interestingly, we found Dock expression was substantially induced following bacterial stimulation, with silencing of the Dock gene in hemocytes resulting in substantially reduced AMPs' expression, ERK phosphorylation, and dorsal translocation, all of which convincingly demonstrate for the first time the critical role played by Dock in innate immunity. More importantly, Dock acted as a bridge to transduce the signaling from the Dscam cytoplasmic tail to ERK in the hemocytes, which contributed immensely to antimicrobial activities. This novel phenomenon indicates Dscam may regulate innate immunity via a Dock-activated signaling pathway that differs with nervous development.

Admittedly, it is difficult to distinguish soluble and membrane-bound Dscam because they share the same outer membrane regions. Yet, nonalternatively spliced exons in the cytoplasmic tail of Dscam provided a good target for us to study the unique functions of membrane-bound Dscam isoforms. In our study, significantly enhanced Dscam expression in crab hemocytes suggests it performs key immune-related functions, as both *in vitro* and *in vivo* experiments demonstrated critical antimicrobial activities of Dscam in the *E. sinensis* crab. We also found that the SH3-binding domain in constant exon 32 translated protein binding with the SH3 domain in Dock, to activate ERK phosphorylation, promoting the phosphorylation and translocation of dorsal, which subsequently enhanced the expression of AMPs. Exon 32 in the cytoplasmic tail was fixed in membrane-bound Dscam; hence, its function in regulating AMPs' expression is likely a common feature of all membrane-bound Dscam isoforms.

For the cytoplasmic tail of Dscam in *E. sinensis* crab, alternatively-spliced exons can generate four isoforms, with the SH2-/SH3-binding domain, endocytosis motif, polyproline motif, and ITIM-like motif in the alternatively and nonalternatively spliced exons. We interpret this as evidence for some conserved functions shared among Dscam cytoplasmic tail isoforms. In particular, the endocytosis motif is located in an alternatively spliced exon, which indicated isoforms with *versus* without this exon may differ considerably in their signaling capacity. The

endocytosis motif is involved in determining the exact site of viral release at the surface of infected mononuclear cells and promotes endocytosis (HAMAP database), which may be linked with the common functions of Dscam-regulated phagocytosis. Building on this premise, we hypothesize that besides the common function of regulating AMPs' expression, isoforms with alternatively spliced exons may have other immune-related functions linked to pathogen-specific recognition capacity of Ig domains in the outer-membrane region of Dscam. If so, this should be able to generate "specific immunity" in invertebrates.

The results from this comprehensive study together demonstrate that Dscam's cytoplasmic tail can generate four isoforms via alternative splicing, with all isoforms able to bind to the SH3 domain in the Dock protein because of the SH3-binding domain in the first constant exon. Dock then promotes ERK phosphorylation via indirect binding, and it regulates dorsal phosphorylation and translocation from the hemocytes' cytoplasm to nucleus. This enables dorsal to regulate the expression of AMPs resulting in the effective clearance of pathogenic bacteria in crab (Fig. 7). Collective data indicate the comprehensive function of Dscam apart from regulating phagocytosis and suggest possible cross-talk occurring between Dscam and other pattern recognition receptors.

Experimental procedures

Study of arthropods and its primary cultured hemocytes

Animal experiments were performed according to a protocol approved by the East China Normal University Animal Care and Use Committee (protocol license number: AR2012/12017), following the animal care guidelines of the Ministry of Science and Technology of the People's Republic of China. Healthy *E. sinensis* crabs (100 ± 10 g per adult, and 15 ± 2 g each for juvenile crabs in a life-stage, nonantibiotic or antifungal fed) were obtained from the Songjiang aquatic farm in Shanghai, China. After quickly transferring them to the Biological Experiment Station at East China Normal University, all crabs were maintained in filtered and aerated freshwater with an abundance of oxygen, and they were fed daily with a commercially-formulated diet free of any antibiotics.

Primary culturing of *E. sinensis* hemocytes was performed according to established techniques (23). More than one hemocyte cell per crab, with multiple crabs used, was isolated and then gently resuspended in Leibovitz's L-15 medium (Sigma) supplemented with 1% antibiotics (10,000 units/ml penicillin, 10,000 µg/ml streptomycin (Gibco)) and 0.2 mM NaCl (676 ± 5.22 mosM/kg), at pH 7.2–7.4, and then counted by an automated cell counter (Invitrogen) before using 4 ml (1 × 10⁶ cells/ml) of it to seed the 60-mm dishes.

Immune stimulation and sample collection

S. aureus bacteria were gifted to us by the National Pathogen Collection Center for Aquatic Animals (Stock No. BYK0113, Shanghai Ocean University, Shanghai, China). Bacteria were cultured, collected, and resuspended in sterile PBS (137 mM NaCl, 2.7 mM KCl, 10 mM Na₂HPO₄, 2 mM KH₂PO₄, pH 7.4). The bacterial counts were determined by plating each diluted suspension onto agar plates.

Dscam controls innate immunity in crab

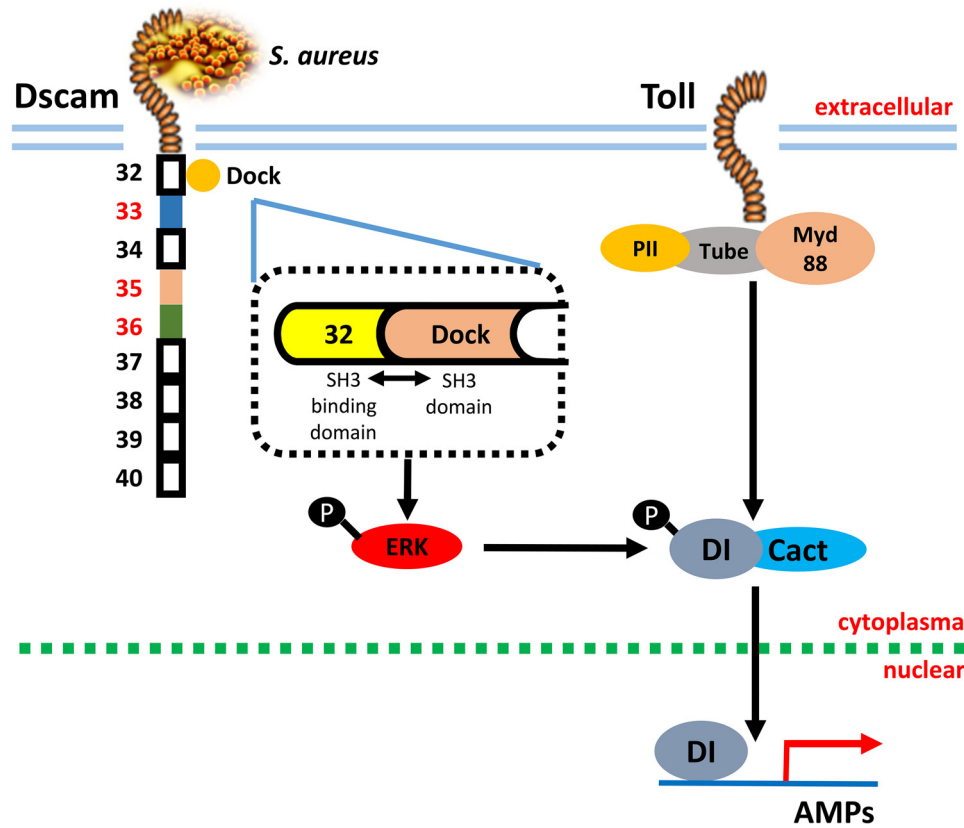


Figure 7. Schematic representation of Dscam-regulated antimicrobial activities in crab. Dscam's cytoplasmic tail can generate four isoforms via alternative splicing, with all isoforms able to bind to the SH3 domain in the Dock protein because of the SH3-binding domain in the first constant exon. Dock then promotes ERK phosphorylation via indirect binding and regulates dorsal phosphorylation and translocation from the hemocyte's cytoplasm to nucleus. This enables dorsal to regulate the expression of AMPs in *E. sinensis* crabs.

For *in vitro* bacterial stimulation, cultured *S. aureus* (1×10^7 microbes per dish, 50 μ l) were added separately to the hemocyte-cultured dish, with sterile PBS (50 μ l) serving as the control. For *in vitro* pathogen associated molecular pattern stimulation, lipopolysaccharide (Sigma) was added separately to a 60-mm dish to a final concentration of 1 μ g/ml, with sterile PBS (50 μ l) as the control. Total RNA was collected from hemocytes at specific time points post-stimulation. At least three crabs were used for each sample. First-strand cDNA was synthesized with a reverse transcriptase kit (Takara, Osaka, Japan) according to the manufacturer's instructions.

For *in vivo* bacterial infection, *S. aureus* (1×10^8 CFU per crab, 200 μ l) were injected into hemolymph from the nonsclerotized membrane of the posterior walking leg, with sterile PBS (200 μ l) used as the control. Total RNA was collected from hemocytes at specific time points post-infection. At least three crabs were used for each sample.

Genomic sequencing, assembly, annotation, and phylogenetic analysis

Total DNA from the muscle of healthy *E. sinensis* was sent to the Novogene Co. (Beijing, China) for whole-genome sequencing on the Illumina HiSeq 2000 and PacBio platforms. The cytoplasmic tail of the *EsDscam* gene sequence was captured from genomic data by alignment and searching within the *EsDscam* cDNA sequence. From genomic data that encoded a protein with SH3 and SH2 domains, a fragment containing a full ORF

was identified and designated as *EsDock*. The full-length *EsDscam* and *EsDock* cDNAs were then each amplified by a pair of gene-specific primers and re-sequenced to confirm the correct sequences. The similarity analysis was conducted using Clustalx from EMBL, with signal peptide(s) predicted by SignalP version 4.1 Server (<http://www.cbs.dtu.dk/services/SignalP/>)⁶ (24) and the domain architecture predicted by SMART (<http://smart.embl-heidelberg.de/>)⁶. The MUSCLE method in MEGA version 6.0 software was used for the alignment of multiple amino acid sequences between the *EsDscam* cytoplasmic tail (ANQ45731.1) and other orthologs of representative pancrustacea in GenBank: *Aedes aegypti* (EAT37388.1); *Apis mellifera* (NP_001014991.1); *Tribolium castaneum* (KYB25260.1); *D. magna* (ACC65887.1); *D. melanogaster* (AF260530.1); *Daphnia pulex* (EFX86769.1); *S. paramamosain* (ANN87808.1); *Pacifastacus leniusculus* (AEC50084.1); and *Cherax quadricarinatus* (AGK90306.1). A nonrooted neighbor-joining phylogenetic tree based on 1000 bootstrap replications was constructed in MEGA version 6.0.

RNAi assay

The cDNA fragments of *EsDscam*, *EsERK*, and *EsDock* were first amplified by PCR with primers linked to the T7 promoter (Table S1, and then were used as the template to produce

⁶ Please note that the JBC is not responsible for the long-term archiving and maintenance of this site or any other third party hosted site.

siRNA with an *in vitro* T7 transcription kit (Fermentas, Burlington, Canada). The corresponding control, GFP dsRNA, was purchased from GenePharma Co. (Shanghai, China). For *in vitro* RNAi, the siRNA was dissolved in RNase-free water and transfected into *E. sinensis* primary-cultured hemocytes using Lipofectamine 3000 (Thermo Fisher Scientific) at a final concentration of 10 nM. For *in vivo* RNAi, the dsRNA (1 µg/g) was injected into the hemolymph from the nonsclerotized membrane of the posterior walking leg of each crab. To strengthen the RNAi effect, a second injection was provided 24 h after the first injection. The efficiency of RNAi was determined via real-time RT-PCR and Western blotting, with dsGFP RNA used as the control. After setting up the RNAi assay, *S. aureus* was used to stimulate the gene-silenced hemocyte *in vitro* or was injected into the gene-silenced crab *in vivo*.

Gene expression profile analysis

The relative expression levels of *EsDscam*, *EsDock*, *EsERK*, and AMP expression in differently-treated hemocytes were determined by real-time RT-PCR using the CFX96™ Real-Time System (Bio-Rad) and SYBR Premix Ex Taq (Tli RNaseH Plus; TaKaRa, Japan) with the primers shown in Table S1. The reaction conditions were 94 °C for 3 min, followed by 40 cycles of 94 °C for 10 s and 60 °C for 1 min, and then melting from 65 to 95 °C. The $2^{-\Delta\Delta CT}$ method was applied to the obtained data, which were normalized to the control group's samples. Three independent experiments were carried out, for which their results as the mean ± S.D. is presented.

Assessment of survival rates and bacterial clearance assay

Sixty crabs were randomly assigned to two groups ($n = 30$ per group). Each crab of the first group was injected with *EsDscam* dsRNA, and 15 µg of GFP dsRNA was injected into crabs of the second group. After *EsDscam* was knocked down by the dsRNA injection, all 60 crabs were injected with *S. aureus* (1×10^9 CFU per crab, 200 µl). The number of dead crabs in each group was recorded daily, and their respective survivorship over 4 days was calculated. Twenty four h after the bacteria injection, the hemolymph from each live crab was collected, diluted, and then cultured on solid LB plates overnight, after which its bacterial colonies were counted.

Western blotting

Protein samples obtained from hemocytes were quantified by the Coomassie Plus Protein Assay Reagent (Thermo Fisher Scientific). Whole-cell lysates were obtained by lysing cells with an RIPA buffer containing protease and phosphatase inhibitor mixtures (Invitrogen). Protein concentration was measured with the Pierce BCA protein assay kit (Thermo Fisher Scientific). Next, the protein was separated by 10% SDS-PAGE and transferred onto a nitrocellulose membrane. This membrane was blocked for 1–2 h with 3% nonfat milk in Tris-buffered saline (TBS: 10 mM Tris-HCl, pH 8.0, 150 mM NaCl) and then incubated with 1:200 diluted antiserum against the proteins of interest, *EsDscam*, *Esp-dorsal*, *EsT-dorsal*, p-ERK, T-ERK, p-JNK, T-JNK, V5, FLAG, Myc, and actin, for 3 h in the same TBS solution after confirming these antibodies generated non-specific signals. After washing three times with TBS, alkaline

phosphatase–conjugated goat anti-rabbit/mouse IgG (1:10,000 diluted in TBS) was added; and following its 3-h incubation with the membrane, any unbound IgG was washed away. The membrane was then dipped into the reaction system and visualized in the dark for 5 min. Antibodies recognizing the phosphorylated forms and total protein of ERK and JNK were purchased from Cell Signaling Technology, and both total protein and antibody-binding sites shared high similarities with these proteins in *E. sinensis*. Antibodies recognizing the phosphorylated forms and total protein of dorsal were produced (WuXi Apptec Co., Wuxi, China) against the specific dorsal protein in *E. sinensis*. Antibodies recognizing the total protein of V5, FLAG, Myc, and actin were purchased from Abcam (Cambridge, UK). All images were collected by the Odyssey CLx (LICOR, Lincoln, NE).

Immunocytochemical staining

To examine ERK phosphorylation and dorsal translocation in crab hemocytes, immunocytochemical staining was applied. Briefly, pretreated hemocytes were blocked with 3% bovine serum albumin (BSA) for 30 min at 37 °C and then incubated overnight at 4 °C with an *EsDorsal* antibody or a p-ERK antibody (1:100 in blocking buffer). After washing with PBS, these hemocytes were incubated with 3% BSA for 10 min, after which the second antibody, goat anti-mouse Alexa Fluor 488 (1:1000 dilution in 3% BSA), was added. The reaction was kept in the dark for 1 h at 37 °C and then washed with PBS. Finally, the hemocytes were stained with '6-diamidino-2-phenylindole dihydrochloride (DAPI, AnaSpec Inc., San Jose) for 10 min at room temperature, washed again, and observed under a Revolve Hybrid Microscope (Echo, San Diego).

Co-immunoprecipitation

For co-IP experiments, human embryonic kidney cells (HEK 293T) were seeded in 60-mm dishes (1×10^7 cells/dish) overnight and transfected with a total of 10 mg of empty plasmid or various expression plasmids. At 48 h post-transfection, the medium was carefully removed, and the cell monolayer washed twice with ice-cold PBS. Then the cells were lysed with 500 ml of RIPA Lysis Buffer (50 mM Tris, pH 7.4, 150 mM NaCl, 1% Nonidet P-40, 0.25% sodium deoxycholate, sodium orthovanadate, sodium fluoride, EDTA, and leupeptin) (Beyotime, Beijing, China) containing a protease mixture (Yeasen, Shanghai, China). Lysates were centrifuged at $14,000 \times g$ for 15 min, and the ensuing supernatant was transferred to a fresh tube and precipitated for 2 h at 4 °C with 30 ml of either an anti-FLAG, anti-V5, or anti-Myc affinity gel (Biotool, Houston, TX). The affinity gel used was washed with cold TBS four times and eluted by boiling for 10 min with TBS and a 6× SDS loading buffer (2% SDS, 60 mM Tris-HCl, pH 6.8, 10% glycerol, 0.001% bromophenol blue, 0.33% β-mercaptoethanol). The cell lysates were also eluted with the same 6× SDS loading buffer and likewise boiled. Proteins isolated from the beads and cell lysates were separated by SDS-PAGE and analyzed by Western blotting using the indicated antibodies. To test the binding between ERK and Dock in crab, 500 µl of hemocytes protein from *E. sinensis* was incubated with *EsERK* or *EsDock* antibody overnight at 4 °C. Protein A/G magnetic beads were added and incu-

Dscam controls innate immunity in crab

bated to capture the antigen–antibody complexes for 3 h at 4 °C. The beads were collected by centrifugation and washed three times with PBS. The mixture was then resuspended with SDS-PAGE loading buffer and boiled at 100 °C for 5 min, subsequently centrifuged again, and analyzed by Western blotting. Purified rabbit IgG was used as a control. Odyssey CLx (LI-COR) instrument was used to collect all the images.

Statements

All authors agree with the submission of this study for publication. This work has not been published or submitted for publication elsewhere, either completely or in part, or in another form or language. No material has been reproduced from another source. Experiments using invertebrate animal were approved by local authorities.

Author contributions—D. L., Z. W., X. L., M. D., and L. Y. software; D. L. and Z. R. validation; D. L., Z. W., and W. L. investigation; D. L., Z. W., X. L., and L. Y. methodology; Z. W. and Z. R. visualization; M. D., Q. W., and W. L. funding acquisition; Q. W. and W. L. supervision; W. L. conceptualization; W. L. data curation; W. L. writing—original draft; W. L. project administration.

Acknowledgments—We thank Prof. Erjun Lin from the Institute of Plant Physiology and Ecology, Chinese Academy of Sciences, for kindly providing cell lines; Dr. Xin Zhang from the Shanghai University of Traditional Chinese Medicine's affiliated Shuguang Hospital for guidance on the co-immunoprecipitation assays; the National Pathogen Collection Center for Aquatic Animals (Shanghai Ocean University, Shanghai, China) for providing us with the bacteria strains; and the Experimental Platform for Molecular Zoology (East China Normal University, Shanghai, China) for providing instruments essential for conducting our study.

References

- Schmucker, D., Clemens, J. C., Shu, H., Worby, C. A., Xiao, J., Muda, M., Dixon, J. E., and Zipursky, S. L. (2000) *Drosophila* Dscam is an axon guidance receptor exhibiting extraordinary molecular diversity. *Cell* **101**, 671–684 [CrossRef Medline](#)
- Watson, F. L., Püttmann-Holgado, R., Thomas, F., Lamar, D. L., Hughes, M., Kondo, M., Rebel, V. I., and Schmucker, D. (2005) Extensive diversity of Ig-superfamily proteins in the immune system of insects. *Science* **309**, 1874–1878 [CrossRef Medline](#)
- Brites, D., McTaggart, S., Morris, K., Anderson, J., Thomas, K., Colson, I., Fabbro, T., Little, T. J., Ebert, D., and Du Pasquier, L. (2008) The Dscam homologue of the crustacean *Daphnia* is diversified by alternative splicing like in insects. *Mol. Biol. Evol.* **25**, 1429–1439 [CrossRef Medline](#)
- Dong, Y., Taylor, H. E., and Dimopoulos, G. (2006) AgDscam, a hypervariable immunoglobulin domain-containing receptor of the *Anopheles gambiae* innate immune system. *PLoS Biol.* **4**, e229 [CrossRef Medline](#)
- Yu, H. H., Yang, J. S., Wang, J., Huang, Y., and Lee, T. (2009) Endodomain diversity in the *Drosophila* Dscam and its roles in neuronal morphogenesis. *J. Neurosci.* **29**, 1904–1914 [CrossRef Medline](#)
- Chou, P. H., Chang, H. S., Chen, I. T., Lee, C. W., Hung, H. Y., and Han-Ching Wang, K. C. (2011) *Penaeus monodon* Dscam (PmDscam) has a highly diverse cytoplasmic tail and is the first membrane-bound shrimp Dscam to be reported. *Fish Shellfish Immunol.* **30**, 1109–1123 [CrossRef Medline](#)
- Black, D. L. (2000) Protein diversity from alternative splicing: a challenge for bioinformatics and post-genome biology. *Cell* **103**, 367–370 [CrossRef Medline](#)
- Wang, E. T., Sandberg, R., Luo, S., Khrebtkova, I., Zhang, L., Mayr, C., Kingsmore, S. F., Schroth, G. P., and Burge, C. B. (2008) Alternative isoform regulation in human tissue transcriptomes. *Nature* **456**, 470–476 [CrossRef Medline](#)
- Azumi, K., De Santis, R., De Tomaso, A., Rigoutsos, I., Yoshizaki, F., Pinto, M. R., Marino, R., Shida, K., Ikeda, M., Arai, M., Inoue, Y., Shimizu, T., Satoh, N., Rokhsar, D. S., et al. (2003) Genomic analysis of immunity in a Urochordate and the emergence of the vertebrate immune system: “waiting for Godot”. *Immunogenetics* **55**, 570–581 [CrossRef Medline](#)
- Du Pasquier, L., Zucchetti, I., and De Santis, R. (2004) Immunoglobulin superfamily receptors in protochordates: before RAG time. *Immunol. Rev.* **198**, 233–248 [CrossRef Medline](#)
- Smith, P. H., Mwangi, J. M., Afrane, Y. A., Yan, G., Obbard, D. J., Ranford-Cartwright, L. C., and Little, T. J. (2011) Alternative splicing of the *Anopheles gambiae* Dscam gene in diverse *Plasmodium falciparum* infections. *Malar. J.* **10**, 156 [CrossRef Medline](#)
- Li, X. J., Yang, L., Li, D., Zhu, Y. T., Wang, Q., and Li, W. W. (2018) Pathogen-specific binding soluble down syndrome cell adhesion molecule (Dscam) regulates phagocytosis via membrane-bound Dscam in crab. *Front. Immunol.* **9**, 801 [CrossRef Medline](#)
- Wojtowicz, W. M., Flanagan, J. J., Millard, S. S., Zipursky, S. L., and Clemens, J. C. (2004) Alternative splicing of *Drosophila* Dscam generates axon guidance receptors that exhibit isoform-specific homophilic binding. *Cell* **118**, 619–633 [CrossRef Medline](#)
- Dong, Y., Cirimotich, C. M., Pike, A., Chandra, R., and Dimopoulos, G. (2012) Anopheles NF- κ B-regulated splicing factors direct pathogen-specific repertoires of the hypervariable pattern recognition receptor AgDscam. *Cell Host Microbe* **12**, 521–530 [CrossRef Medline](#)
- Valanne, S., Wang, J. H., and Rämetsä, M. (2011) The *Drosophila* Toll signaling pathway. *J. Immunol.* **186**, 649–656 [CrossRef Medline](#)
- Sun, J. J., Lan, J. F., Shi, X. Z., Yang, M. C., Niu, G. J., Ding, D., Zhao, X. F., Yu, X. Q., and Wang, J. X. (2016) β -Arrestins negatively regulate the Toll pathway in shrimp by preventing dorsal translocation and inhibiting dorsal transcriptional activity. *J. Biol. Chem.* **291**, 7488–7504 [CrossRef Medline](#)
- Neves, G., Zucker, J., Daly, M., and Chess, A. (2004) Stochastic yet biased expression of multiple Dscam splice variants by individual cells. *Nat. Genet.* **36**, 240–246 [CrossRef Medline](#)
- Graveley, B. R. (2005) Mutually exclusive splicing of the insect Dscam pre-mRNA directed by competing intronic RNA secondary structures. *Cell* **123**, 65–73 [CrossRef Medline](#)
- Armitage, S. A., Freiburg, R. Y., Kurtz, J., and Bravo, I. G. (2012) The evolution of Dscam genes across the arthropods. *BMC Evol. Biol.* **12**, 53 [CrossRef Medline](#)
- Hattori, D., Millard, S. S., Wojtowicz, W. M., and Zipursky, S. L. (2008) Dscam-mediated cell recognition regulates neural circuit formation. *Annu. Rev. Cell Dev. Biol.* **24**, 597–620 [CrossRef Medline](#)
- Clemens, J. C., Ursuliak, Z., Clemens, K. K., Price, J. V., and Dixon, J. E. (1996) A *Drosophila* protein-tyrosine phosphatase associates with an adapter protein required for axonal guidance. *J. Biol. Chem.* **271**, 17002–17005 [CrossRef Medline](#)
- Rao, Y., and Zipursky, S. L. (1998) Domain requirements for the Dock adapter protein in growth-cone signaling. *Proc. Natl. Acad. Sci. U.S.A.* **95**, 2077–2082 [CrossRef Medline](#)
- Zhu, Y., Jin, X., Fang, Z., Zhang, X., Li, D., Li, W., and Wang, Q. (2015) A novel *Eriocheir sinensis* primary hemocyte culture technique and its immunoreactivity after pathogen stimulation. *Aquaculture* **446**, 140–147 [CrossRef](#)
- Nielsen, H. (2017) Predicting secretory proteins with SignalP. *Methods Mol. Biol.* **1611**, 59–73 [CrossRef Medline](#)

Alternatively spliced down syndrome cell adhesion molecule (Dscam) controls innate immunity in crab

Dan Li, Zhicheng Wan, Xuejie Li, Ming Duan, Lei Yang, Zechao Ruan, Qun Wang and Weiwei Li

J. Biol. Chem. 2019, 294:16440-16450.

doi: 10.1074/jbc.RA119.010247 originally published online September 19, 2019

Access the most updated version of this article at doi: [10.1074/jbc.RA119.010247](https://doi.org/10.1074/jbc.RA119.010247)

Alerts:

- [When this article is cited](#)
- [When a correction for this article is posted](#)

[Click here](#) to choose from all of JBC's e-mail alerts

This article cites 24 references, 6 of which can be accessed free at <http://www.jbc.org/content/294/44/16440.full.html#ref-list-1>